

## High Energy Scales in the Optical Self-Energy of the Cuprate Superconductors

J. Hwang,<sup>1</sup> E. J. Nicol,<sup>2</sup> T. Timusk,<sup>1,3</sup> A. Knigavko,<sup>4</sup> and J. P. Carbotte<sup>1,3</sup>

<sup>1</sup>*Department of Physics and Astronomy, McMaster University, Hamilton, Ontario N1G 2W1, Canada*

<sup>2</sup>*Department of Physics, University of Guelph, Guelph, Ontario N1G 2W1, Canada*

<sup>3</sup>*The Canadian Institute of Advanced Research, Toronto, Ontario M5G 1Z8, Canada*

<sup>4</sup>*Department of Physics, Brock University, St. Catharines, Ontario L2S 3A1, Canada*

(Received 17 October 2006; published 18 May 2007)

Using optical spectroscopy with a derivative technique, we find for the high  $T_c$  cuprate  $\text{Bi}_2\text{Sr}_2\text{CaCu}_2\text{O}_{8+\delta}$  (Bi-2212) evidence for a new high energy scale at 900 meV beyond the two previously well-known ones at roughly 50 and 400 meV. The intermediate scale at 400 meV has recently been seen in angle-resolved photoemission spectroscopy experiments along the nodal direction as a large kink. In  $\text{YBa}_2\text{Cu}_3\text{O}_{6.50}$ , the three energy scales are shifted to lower energy relative to Bi-2212 and we observe the emergence of a possible new high energy feature at 600 meV.

DOI: [10.1103/PhysRevLett.98.207002](https://doi.org/10.1103/PhysRevLett.98.207002)

PACS numbers: 74.25.Gz, 74.20.Mn, 74.72.-h

One of the most beautiful aspects of studying condensed matter systems is that a large number of very different types of experiments are available to probe the many-body state, and in the quest for microscopic understanding all of the various probes must concur about the features observed. This provides a stringent test of theories and further allows for the perfection of experimental technique and analysis. Consequently, if there is an opportunity to bring two different techniques closer together for the purpose of comparison, both theory and experiment will benefit and there will be a great enhancement of the ability to identify fundamental and robust signatures of the underlying physics. Two powerful techniques which have been brought to bear on the problem of high  $T_c$  superconductivity are angle-resolved photoemission spectroscopy (ARPES) [1,2] and far-infrared optical spectroscopy [3]. These techniques have blossomed with the demands of this area, resulting in unprecedented resolution and new methods for extraction and analysis of information, such as through inversion techniques [4–9].

The result of the optical techniques has been the identification of a coupling of the charge carriers to a resonance mode at about 50 meV and a spin-fluctuation background extending beyond 400 meV [8–11]. Until very recently, ARPES experiments on cuprate materials were limited to presenting high resolution data for the quasiparticle dispersion curve only up to about 200–300 meV in energy [12–16]. However, new advances have extended this range to greater than 1 eV and several works [17–21] are reporting features at high energy at about 400 and 800 meV, which are speculated to arise from exotic physics. Confirming the existence of these new energy scales and investigating a wide range of materials are essential to the development of these or other new ideas. Indeed, another ARPES group [22,23] has commented on the vertical dispersion seen in the data from 400 to 800 meV and, based on further experimental work, has suggested that this feature may be associated with matrix element effects which

are highly momentum dependent and can suppress photoemission intensity near the Brillouin zone center. Clearly, this controversy necessitates an independent probe via another experimental technique.

In this Letter, we present new evidence for the existence of high energy scales revealed from optical conductivity data. This is important because optics is a bulk probe as opposed to ARPES which is only sensitive to the surface. In addition, optical spectroscopy measures the self-energy due to correlations directly while ARPES finds, instead, the renormalized dispersion. The self-energy follows only once the bare dispersion is known. Using a derivative technique to analyze the data on  $\text{Bi}_2\text{Sr}_2\text{CaCu}_2\text{O}_{8+\delta}$  (Bi-2212) samples of varying doping, we can show that optics sees features at high energy and supports some of the observations seen in ARPES, but not all. Moreover, as optical experiments are more flexible in the type of materials which can be studied, our work goes beyond Bi-2212 to examine the high energy scales in  $\text{YBa}_2\text{Cu}_3\text{O}_{6.50}$  (YBCO). Having established scales in a model-independent way, we use a boson exchange model to further extract from the data an approximation to the quasiparticle self-energy which we then use to compare directly with ARPES.

Within the experimental community, it has become common to analyze the complex optical conductivity  $\sigma(\omega)$  for correlated charge carriers in terms of the optical self-energy,  $\Sigma^{\text{op}} = \Sigma_1^{\text{op}}(\omega) + i\Sigma_2^{\text{op}}(\omega)$ , using an extended Drude model of the form [3,10]  $4\pi\sigma(\omega) = i\omega_p^2/[\omega - 2\Sigma^{\text{op}}(\omega)]$ , where  $\omega_p$  is the plasma frequency. We note that  $\Sigma^{\text{op}}$  is not the quasiparticle self-energy  $\Sigma^{\text{qp}}$ . However,  $\Sigma^{\text{op}}$  does encode such information as it depends on an integral over a function of the quasiparticle self-energy. This fact suggests using a derivative technique to relate more directly the conductivity to structures in the quasiparticle renormalizations. A natural choice is to consider the first derivative of  $\omega\Sigma^{\text{op}}(\omega)$  [denoted here by  $\Sigma^{\text{op-qp}}(\omega) \equiv d[\omega\Sigma^{\text{op}}(\omega)]/d\omega$ ] as we will clarify later when we consider more specific models. For the moment,

we proceed without appealing to any particular theory of highly correlated systems.

We now present our new results on high energy scales in three Bi-2212 systems: underdoped (UD69), optimally-doped (OPT96), and overdoped (OD60), and one underdoped YBCO material (UD59) taken from the existing literature [10,24,25] as imaged by optics. To obtain  $\Sigma^{\text{op}}$  from the optical conductivity we have to know two quantities,  $\epsilon_H$  and  $\omega_p$ , which are the contribution to the dielectric constant from high frequencies above the charge transfer gap and the plasma frequency, respectively. Estimation of these two values is discussed in the literature [24] and for the three Bi-2212: UD69 ( $\epsilon_H = 4.0$ ,  $\omega_p = 18980 \text{ cm}^{-1}$ ), OPT96 (4.32, 19 500), and OD60 (5.14, 21 140), and for the YBCO UD59 (4.34, 17 490). Here we have used a rather high  $\omega_p$  and there is no crossing with the frequency axis of the real part of  $\Sigma^{\text{op}}(\omega)$ . However, the existence of crossing is an issue of debate.

The derivative needed to obtain  $\Sigma^{\text{op-qp}}$  can magnify the noise in the experimental data. To remove this artificial noise and capture the global features, which is all we are interested in, we applied an ‘‘adjacent-point-averaging smoothing process’’ with 20 adjacent data points with a window of roughly 2 meV. Independently, we fitted  $\omega\Sigma^{\text{op}}(\omega)$  with a 10-term polynomial and differentiated the fitted curve to obtain  $\Sigma^{\text{op-qp}}(\omega)$ . We compared the two results and found that they are consistent with each other as is shown in Fig. 1(c), where polynomial fit (dashed line) and adjacent point averaging (solid line) are shown for both real [light gray (red)] and imaginary [dark gray (blue)] parts. Both methods give almost the same results.

In Fig. 1(a), we show results for  $-\Sigma_1^{\text{op-qp}}$ . For the Bi-2212 samples we have indicated possible features that would correlate with the  $E_0$ ,  $E_1$ , and  $E_2$  seen in ARPES providing possible confirmation of three similar energy scales seen universally across members of the Bi-2212 family. For the YBCO sample, we also can suggest the existence of the three energy scales. While  $E_0$  remains the same, the  $E_1$  and  $E_2$  scales are now shifted to lower energy relative to Bi-2212 and are labeled  $E'_1$  (not shown) and  $E'_2$ . In addition, there is a possible fourth scale,  $E'_3 \sim 0.6 \text{ eV}$ . In Fig. 1(b), we show  $-\Sigma_2^{\text{op-qp}}$  of the four samples. The imaginary quantity,  $-\Sigma_2^{\text{op-qp}}$ , is positive definite and also shows the characteristic energy scales. In particular, we see the emergence of a new band at larger energy. In the case of a finite band, we expect the scattering rate to drop [26–28] beyond the end of the boson spectrum. We note that the data used to obtain the curves in Fig. 1(a) and 1(b) were separately smoothed before differentiation. The fact that both sets of curves give the same values for the energy scales confirms that these estimates are a robust feature of the data. Of course the signature of the various energy scales is not the same in the real and imaginary parts of  $\Sigma^{\text{op-qp}}$ . For instance, there is a peak in the real part at  $E_0$ , while the imaginary part shows an abrupt change in its rate

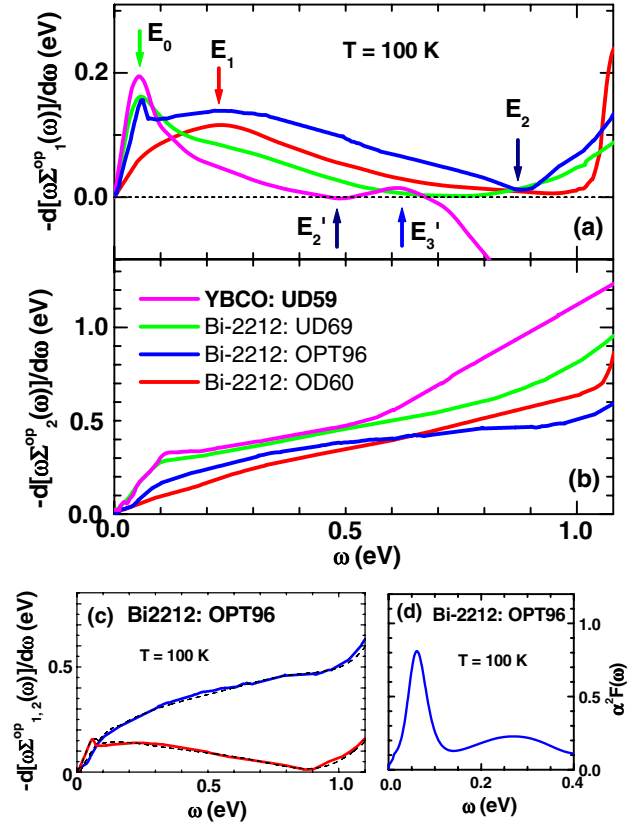


FIG. 1 (color online). (a) The real part of  $-d[\omega\Sigma_1^{\text{op}}(\omega)]/d\omega$  for three Bi-2212 samples, overdoped, optimally doped, and underdoped, and one underdoped YBCO in the orthoII phase [25], all at  $T = 100 \text{ K}$ . (b) Its imaginary part. Various energy scales are indicated and discussed in the text. (c) shows  $-d[\omega\Sigma_1^{\text{op}}(\omega)]/d\omega$  using a polynomial fit (dashed line) and adjacent point averaging (solid line). (d) gives the  $\alpha^2F(\omega)$  obtained in Bi-2212 from inversion of optical data [11]. Note the clear signature of the  $E_1$  scale in this function.

of increase. The  $E_1$  scale is a peak or shoulder in the top frame and a near linear region in the bottom frame. The  $E_2$  scale corresponds in both cases to a rapid increase (decrease in one case) in the curves.

To provide a more detailed comparison with ARPES data, we need to consider some specific microscopic model. What we have done so far is model independent. If we assume, for the sake of argument, that the optical self-energy of charge carriers is due to some sort of frequency-dependent interaction with a bosonic spectrum which we will call  $\alpha^2F(\omega)$ , then [26–29]

$$-2\Sigma_1^{\text{op}}(\omega) \simeq \frac{2}{\omega} \int_0^\infty d\Omega \alpha^2F(\Omega) \int_0^\infty d\omega' \tilde{N}(\omega') \times \ln\left(\frac{[\omega' + \Omega]^2}{[\omega' + \Omega]^2 - \omega^2}\right), \quad (1)$$

$$-2\Sigma_2^{\text{op}}(\omega) \simeq \frac{2\pi}{\omega} \int_0^\infty d\Omega \alpha^2F(\Omega) \int_0^{\omega-\Omega} d\omega' \tilde{N}(\omega'), \quad (2)$$

where the effective renormalized electronic density of states  $\tilde{N}(\omega)$  can be energy dependent. The approximations behind these formulas and their range of validity may be found in [30–32]. These equations are stated here for  $T = 0$  and for no impurity scattering. In the cuprates, we can assume the clean limit. Finite temperature effects are easily incorporated when needed. Differentiation of Eqs. (1) and (2) after multiplication by  $\omega$  shows that for this case  $\Sigma^{\text{op-qp}}$  is just the quasiparticle self-energy which suggests we use  $\Sigma^{\text{op-qp}}$  in any comparison with dispersion curves.

To illustrate the effectiveness of this method, we show results of a model calculation in Fig. 2, where an  $\alpha^2 F(\omega)$  spectrum consisting of three delta functions has been used to calculate both the exact  $\Sigma^{\text{qp}}$  from many-body theory and the optical conductivity in the usual Kubo approximation [26,27]. The optical conductivity is then processed via the extended Drude model to obtain  $\Sigma^{\text{op-qp}}$ . In the figure, we plot the real part of  $\Sigma^{\text{qp}}$  which shows very clearly three structures due to the three  $\delta$ -function peaks in the  $\alpha^2 F$  at 0.04, 0.09, and 0.19 eV [27]. However, the curve formed from  $\Sigma^{\text{op}}$  is almost featureless and does not capture the underlying structure of the spectral function. In addition, this calculation has included a finite band density of states [26–28] which causes the renormalized dispersion curve to cross the bare dispersion curve and once again the curve from  $\Sigma^{\text{op}}$  has not crossed the bare dispersion at the right energy. On the other hand,  $\Sigma^{\text{op-qp}}$  is in good agreement with the exact one and it reproduces all of the structures at

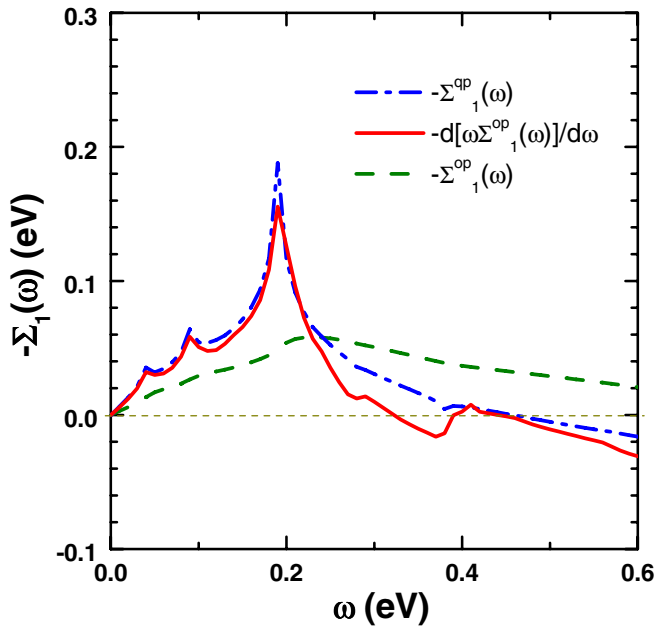


FIG. 2 (color online). Demonstration that an image of the quasiparticle self-energy can be extracted from optics (solid red curve) via the derivative of  $\omega \Sigma^{\text{op}}$ . It agrees well in magnitude and detailed structure with the exact theoretical curve for  $\Sigma^{\text{qp}}$  (dash-dotted blue). The optical self-energy curve (dashed green) is almost structureless and does not agree with the  $\Sigma^{\text{qp}}$  curve.

the correct energies and with the proper magnitude. Aside from a small overshoot of the curve between about 0.3 and 0.4 eV due to the derivative technique which is known to produce such characteristics just after the end of a sharp boson spectrum (negligible for a smooth spectrum [33]), the op-qp curve also crosses the bare dispersion at the same point as the qp curve. The agreement is remarkable. It is clear from this figure that  $\Sigma^{\text{op-qp}}$  is to be used rather than  $\Sigma^{\text{op}}$  in any serious comparison with dispersion curves. However, we stress that the “dispersion curves” presented here are to be viewed as momentum-averaged curves in terms of the self-energy and the only remaining momentum dependence enters through the bare dispersion  $\epsilon_k$ .

Near the Fermi surface the bare dispersion is  $E_k = \epsilon_k \approx v_F(k - k_F)$ , where  $v_F$  is the Fermi velocity, which we obtain from the local density approximation calculation (LDA) [34], and  $k_F$  is the wave vector at the Fermi surface. In Fig. 3(a) we show a color map of the quasiparticle spectral function:  $A(k, \omega) = \frac{1}{\pi} |\Sigma_2^{\text{op-qp}}(\omega)| / [(\omega - v_F(k - k_F) - \Sigma_1^{\text{op-qp}}(\omega))^2 + (\Sigma_2^{\text{op-qp}}(\omega))^2]$ . In Fig. 3(b), we compare our data with that of Graf *et al.* [17] from ARPES in the nodal direction on a similar optimally doped sample. In ARPES, they identify three energy scales at  $E_0 \sim 50$  meV,  $E_1 \sim 0.4$  eV, and  $E_2 \sim 0.8$  eV. In our data, we can confirm a structure at  $E_2 \sim 0.9$  eV and a much stronger kink at  $E_0 \sim 50$  meV; however, we find a local maximum around 0.25 eV, which may be consistent with the 0.40 eV in ARPES seen along the nodal direction if we consider the possible  $k$  dependence of this kink [21] and  $k$  average of

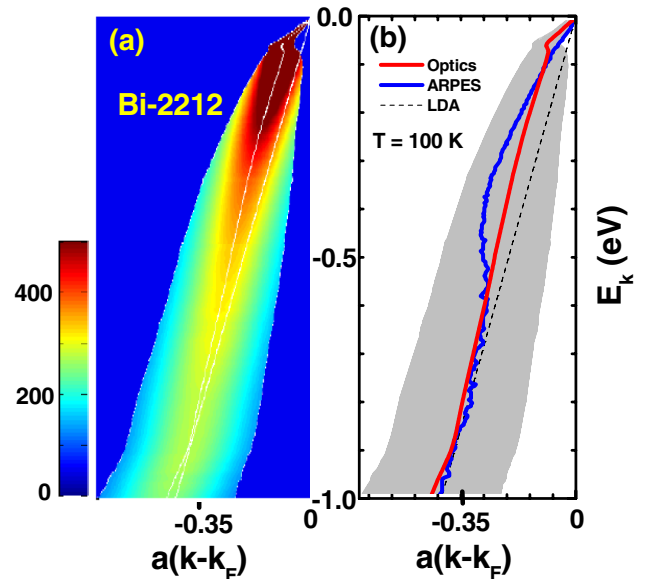


FIG. 3 (color online). (a) Dispersion curve derived from optics for optimally doped Bi-2212, in a color map as is done in ARPES. Here  $a$  is the lattice constant. (b) Maxima points in the momentum dispersion curve (MDC),  $E_k = v_F(k - k_F) + \Sigma_1^{\text{op-qp}}(E_k)$ , compared with ARPES [17] and with LDA Ref. [34],  $E_k = \epsilon_k \approx v_F(k - k_F)$ . The gray shading gives the full width at the half maximum of the MDC curve  $\Sigma_2^{\text{op-qp}}(E_k)$ .

optical data. The energy scale of the 0.4 eV kink has been seen to change gradually from zero in the antinodal to its maximum in the nodal direction in the optimally doped  $\text{La}_{1.83}\text{Sr}_{0.17}\text{CuO}_4$  (LSCO) system [21]. The broadening that we find is also within the range found by ARPES. Thus, we conclude that overall we find reasonable agreement with ARPES using our analysis as shown in Fig. 3(b).

Inversion [8,9] of optical data to recover the electron-boson spectral density of Eqs. (1) and (2) shows that the kink at  $\sim 50$  meV can be attributed to a peak in  $\alpha^2F(\omega)$  which is followed by a broad spin-fluctuation background extending beyond 0.4 eV [see Fig. 1(d)]. This spectrum accounts for the deviations, extending up to  $\sim 0.6$  eV, of the op-qp data from the LDA curve seen in Fig. 3(b). The renormalization found in the ARPES data, while larger than that found in the op-qp curve around 0.4 eV, is smaller below the 50 meV kink. The lack of quantitative agreement between the optics and ARPES in these two regions may reflect (i) the differences between the quasiparticle and transport spectral densities, not included in this work, (ii) the differences in  $k$  dependence between optical data (averaged over the Fermi surface) and that of ARPES (momentum specific), and (iii) that formally the self-energy  $\Sigma(\mathbf{k}, \omega)$  can depend on the magnitude of  $\mathbf{k}$  as well as direction, but this goes beyond the theory used here. It is clear that renormalizations are present in both experiments on a broad energy scale up to the end of the spin-fluctuation spectrum ( $\sim 0.4$  eV), which we take here to be the  $E_1$  scale rather than the position of a peak in the self-energy. Furthermore, we associate the higher energy scale around 0.8–0.9 eV with the termination of the first band, followed by the commencement of a new higher energy band. One result, strongly highlighted in some of the ARPES work [19,20], is the vertical dispersion seen in the data from  $E_1$  to  $E_2$ . The question arises as to whether this is due to some sort of ordering [19,20] or if it is a renormalization effect, or indeed a problem associated with the ARPES matrix element [22,23]. A vertical dispersion can be obtained within standard electron-boson models [28,35] with appropriate choice of parameters and, in this instance, the high energy scale of this feature points to a spin-fluctuation spectrum rather than a low energy boson. Thus, we would conclude that the large kink is due to renormalization rather than something more exotic, as was also concluded by Valla *et al.* [19].

In summary, we have used a first derivative of  $\omega$  times the optical self-energy to establish the various energy scales present in renormalization effects. In Bi-2212 at various dopings, we find good agreement with the ARPES data in comparison with the optically derived quasiparticle dispersion curve. While the optics data show features at both low and high energies ( $E_0 \sim 50$  meV and  $E_2 \sim 0.9$  eV) as in ARPES, the profile of the intermediate scale  $E_1 \sim 0.4$  eV, which we identify as the background spin-fluctuation scale, is very different in

optics, possibly because there is no momentum resolution. Nevertheless, optics provides a complementary technique to ARPES both due to its enhanced energy resolution and its ability to examine a wider range of materials such as the YBCO family. Indeed, we find in YBCO that we can identify up to four energy scales, but that overall these scales appear to be shifted to lower energy relative to Bi-2212. The theoretical understanding of these features remains to be more fully elucidated, but confirmation of these scales by more than one technique gives impetus to such an endeavour.

This work has been supported by the Natural Science and Engineering Council of Canada (NSERC) and the Canadian Institute for Advanced Research (CIAR).

- 
- [1] C. Campuzano *et al.*, in *Physics of Conventional and Unconventional Superconductors*, edited by K. H. Bennemann and J. B. Ketterson (Springer-Verlag, Berlin, 2003), Vol. 2, p. 167.
  - [2] A. Damascelli *et al.*, *Rev. Mod. Phys.* **75**, 473 (2003).
  - [3] D. N. Basov *et al.*, *Rev. Mod. Phys.* **77**, 721 (2005).
  - [4] X. J. Zhou *et al.*, *Phys. Rev. Lett.* **95**, 117001 (2005).
  - [5] S. Verga *et al.*, *Phys. Rev. B* **67**, 054503 (2003).
  - [6] F. Marsiglio *et al.*, *Phys. Lett. A* **245**, 172 (1998).
  - [7] S. V. Dordevic *et al.*, *Phys. Rev. B* **71**, 104529 (2005).
  - [8] E. Schachinger *et al.*, *Phys. Rev. B* **73**, 184507 (2006).
  - [9] J. P. Carbotte *et al.*, *Nature (London)* **401**, 354 (1999).
  - [10] J. Hwang *et al.*, *Nature (London)* **427**, 714 (2004).
  - [11] J. Hwang *et al.*, *Phys. Rev. B* **75**, 144508 (2007).
  - [12] A. Kaminski *et al.*, *Phys. Rev. Lett.* **86**, 1070 (2001).
  - [13] T. Sato *et al.*, *Phys. Rev. Lett.* **91**, 157003 (2003).
  - [14] A. A. Kordyuk *et al.*, *Phys. Rev. Lett.* **97**, 017002 (2006).
  - [15] T. K. Kim *et al.*, *Phys. Rev. Lett.* **91**, 167002 (2003).
  - [16] P. D. Johnson *et al.*, *Phys. Rev. Lett.* **87**, 177007 (2001).
  - [17] J. Graf *et al.*, *Phys. Rev. Lett.* **98**, 067004 (2007).
  - [18] B. P. Xie *et al.*, *Phys. Rev. Lett.* **98**, 147001 (2007).
  - [19] T. Valla *et al.*, *Phys. Rev. Lett.* **98**, 167003 (2007).
  - [20] J. Graf *et al.*, arXiv:cond-mat/0610313.
  - [21] J. Chang *et al.*, arXiv:cond-mat/0610880 [Phys. Rev. B (to be published)].
  - [22] A. A. Kordyuk *et al.*, arXiv:cond-mat/0702374.
  - [23] D. S. Inosov *et al.*, arXiv:cond-mat/0703223.
  - [24] J. Hwang *et al.*, *J. Phys. Condens. Matter* **19**, 125208 (2007).
  - [25] J. Hwang *et al.*, *Phys. Rev. B* **73**, 014508 (2006).
  - [26] A. Knigavko *et al.*, *Phys. Rev. B* **72**, 035125 (2005).
  - [27] A. Knigavko *et al.*, *Phys. Rev. B* **73**, 125114 (2006).
  - [28] E. Cappelluti *et al.*, *Phys. Rev. B* **68**, 224511 (2003).
  - [29] B. Mitrović *et al.*, *Phys. Rev. B* **31**, 2694 (1985).
  - [30] P. B. Allen, *Phys. Rev. B* **3**, 305 (1971).
  - [31] S. V. Shulga *et al.*, *Physica (Amsterdam)* **178C**, 266 (1991).
  - [32] S. G. Sharapov *et al.*, *Phys. Rev. B* **72**, 134506 (2005).
  - [33] J. P. Carbotte *et al.*, *Phys. Rev. B* **71**, 054506 (2005).
  - [34] Hsin Lin *et al.*, *Phys. Rev. Lett.* **96**, 097001 (2006).
  - [35] E. Schachinger *et al.*, *Phys. Rev. B* **67**, 214508 (2003).